ARMA 21–1799

Three-Dimensional Anisotropic Shear Strength of Jointed Rock Masses

Cylwik, S.D.
Call & Nicholas, Inc., Tucson, AZ, USA

Copyright 2021 ARMA, American Rock Mechanics Association

This paper was prepared for presentation at the 55th US Rock Mechanics/Geomechanics Symposium held in Houston, Texas, USA, 20-23 June 2021. This paper was selected for presentation at the symposium by an ARMA Technical Program Committee based on a technical and critical review of the paper by a minimum of two technical reviewers. The material, as presented, does not necessarily reflect any position of ARMA, its officers, or members. Electronic reproduction, distribution, or storage of any part of this paper for commercial purposes without the written consent of ARMA is prohibited. Permission to reproduce in print is restricted to an abstract of not more than 200 words; illustrations may not be copied. The abstract must contain conspicuous acknowledgement of where and by whom the paper was presented.

ABSTRACT: This study combines novel and previously published data to create a new method of estimating anisotropic rock-mass strength in three dimensions that considers both the orientation and the non-persistence of multiple joint sets. Equations are developed to evaluate joint persistence as a function of joint set spacing-to-length ratio, strength reduction as a function of joint persistence, and strength reduction as a function of dip and dip direction difference between a joint set and the shear plane. Vector rotations are used to calculate the dip and dip direction difference between the orientations of joint sets and the assumed shear plane orientation, allowing anisotropic rock-mass shear strength to be estimated for any three-dimensional direction of shear. The result is reduced strength for shear in the directions parallel to jointing and increased strength for shear in directions non-parallel to jointing, with a continuous function of strength in between the two extremes. Input parameters for the system are rock discontinuity set statistics, intact rock strength, discontinuity strength, and RQD. A slope instability case history example is back analyzed using the strength estimation procedure. A calculation sheet that implements the methodology is presented and shared for digital download.

1. INTRODUCTION

Most rock-mass slope failures involve some structural component. For large rock slope failures, several sets of non-persistent sets of joints may interact with intact blocks of rock to form a combined shear plane. Anisotropic analysis of a shear plane parallel to continuous jointing is straightforward, but a practical and accessible methodology to analyze anisotropic strength of a rock mass with multiple non-continuous joint sets remains elusive.

There are many factors that contribute to the ultimate strength of a rock-mass shear plane including: the strength of the joints and the intact rock, the orientation of joints relative to the shear plane, and the persistence of the joints. It is difficult if not impossible to measure rock-mass strength directly or to quantify these factors independently. Physical models and numerical models provide a more reasonable approach, and many studies have been performed in recent years with promising results.

This research combines novel and previously published data to create a new method of estimating anisotropic rock-mass strength in three dimensions that considers both the orientation and the non-persistence of multiple joint sets. To make the system easy to implement in day-to-day rock engineering problems, the input parameters are limited to rock discontinuity set statistics, intact rock strength, discontinuity strength, and RQD. To create the system, the following relations are developed:

- Joint persistence as a function of joint set spacing-to-length ratio
- Strength reduction as a function of joint persistence
- Strength reduction as a function of dip and dip direction difference between a joint set and the shear plane
- A methodology to calculate the dip and dip direction difference between the anisotropy orientation and the shear plane
- A methodology to combine the two separate strength reduction factors

2. DEVELOPMENT OF RELATIONS

2.1. Joint Persistence as a Function of Joint Set Spacing-to-Length Ratio

Fracture network simulation software was used to generate simulated two-dimensional fracture networks with various spacing-to-length ratios, with the assumption that both joint set spacing and length follow the negative

exponential distribution. Simulated shear paths sub-parallel to jointing were created and the percentage rock bridge required to create the shear path was measured. The percentage intact rock bridge along each shear path, B_r, was measured using Eq. (1), where L_r is the rock bridge length and L_j is the joint length. An example fracture network simulation and shear path is shown in Figure 1. Eq. (2) was developed to fit the data and relate joint set spacing-to-length ratio to the percentage rock bridge along the shear path for spacing-to-length ratios less than 1, as shown in Figure 2.

$$B_r = \frac{L_r}{L_r + L_j} \quad (1)$$

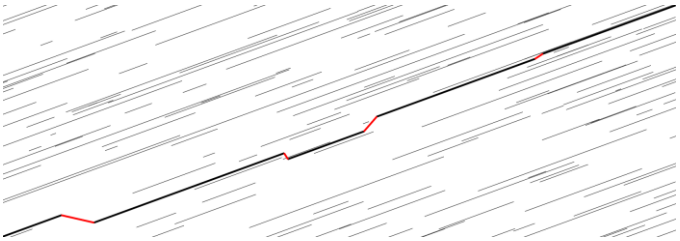

Fig. 1. Example fracture network with optimized shear path (red represents rock bridge), spacing-to-length ratio=0.13.

$$B_r = 1 - 0.5^{\frac{Spacing}{Length}} \quad (2)$$

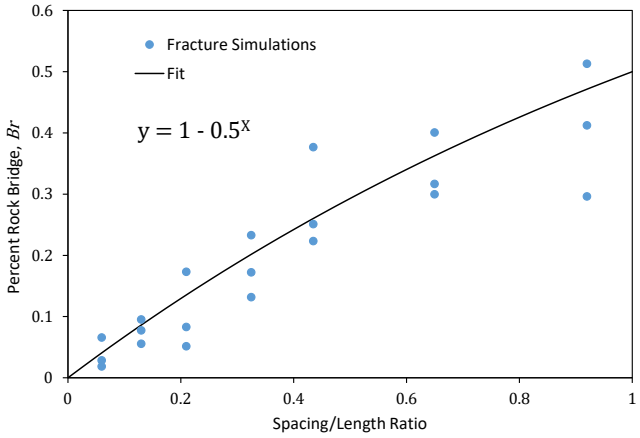

Fig. 2. Discontinuity spacing-to-length ratio versus measured percent intact rock bridge.

2.2. *Strength Reduction as a Function of Joint Persistence*

The data from six studies were used to develop a relation for strength reduction as a function of joint persistence. Modeled or simulated jointing was non-continuous for all the studies. Strength reduction (R_{JR}) was modeled as the percentage reduction between the joint/discontinuity strength (τ_j) and the intact rock strength (τ_i) as shown in Eq. (3), similar to the Jennings (1972) criteria. Data were transformed to shear-normal space to aid in direct comparison. Shaunik and Singh (2019) and Cheng et al. (2016) constructed plaster specimens with non-persistent joints and tested them under uniaxial stress. Bahaaddini et al. (2013, 2016) used calibrated PFC3D models to predict the effect of non-persistent joints on uniaxial strength. Fereshtenejad (2020) used 3D printing and casting technology to build plaster specimens with co-planar intermittent joints and tested them in direct shear. Hu et al. (2020) constructed cement mortar samples with discontinuous fractures and conducted direct shear tests. Eq. (4) was developed to fit the data and relate percentage rock bridge along the shear path to a linear strength weighting reduction factor as shown in Figure 3.

$$\tau = R_{JR} * \tau_i + \left(1 - R_{JR}\right) * \tau_j \quad (3)$$

$$R_{JR} = {B_r}^{1.5} \quad (4)$$

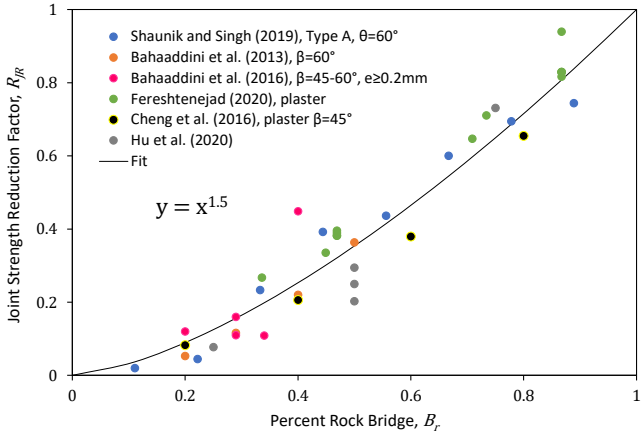

Fig. 3. Percent rock bridge versus strength reduction factor.

The probability of joint set occurrence (P_O) may be combined with Eqs. (2) and (4) resulting in Eq. (5) that estimates the strength reduction factor (R_J) for sliding parallel to jointing based spacing, length, and P_O. The P_O of a joint set is determined by terrestrial- or photogrammetry-based cell mapping (Nicholas and Sims, 2000), and is defined as the percentage of cells in which a joint set is observed. An example of calculated reduction factors using Eq. 5 is shown in Table 1.

$$R_J = 1 - P_O * (1 - (1 - 0.5^{\frac{Spacing}{Length}})^{1.5}) \quad (5)$$

Table 1. Example Calculated Strength Reduction Factors, R_J

	Prob.of Occurrence, P_O	Mean Length (ft/m)	Mean Spacing (ft/m)	Strength Reduction Due to Jointing (R_J)
Joint Set 1	1.00	18.6	5.8	0.09
Joint Set 2	0.45	20.0	4.2	0.57
Joint Set 3	0.33	11.1	1.2	0.68
Joint Set 4	0.90	13.3	8.3	0.28

2.3. *Strength Reduction as a Function of Orientation Difference*

The data from two studies were used to develop a relation for strength reduction as a function of orientation

difference between the shear plane and the plane of anisotropy. Lit et al. (2014) performed laboratory shear tests on rock-mass models containing two joint sets (one continuous), and a DEM model was also used to simulate the tests. Ghazvinian (2013) used an oblique shear apparatus to test inherently anisotropic core samples, and the core was cut at various angles and rotated to various angles to test different anisotropy orientations relative to the shear plane. For both studies, the anisotropy was continuous. Eq. (6) was developed to fit the data and relate the difference in dip (ΔDip) and dip direction (ΔDDR) between the shear plane and the anisotropy direction to a linear strength weighting reduction factor, R_D, as shown in Figure 4.

$$R_D = 1 - \cos(\Delta Dip)^{[3*\sin(\Delta DDR)^{1.5}+1.7]} \quad (6)$$

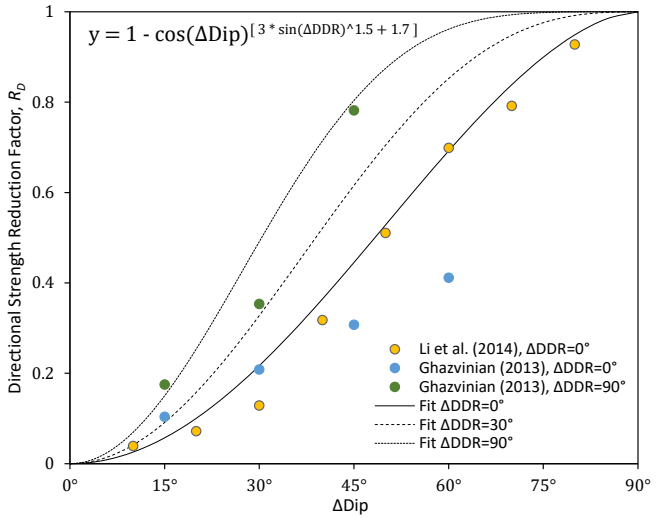

Fig. 4. Dip difference and dip direction difference versus strength reduction factor.

2.4. *Calculation of ΔDip and ΔDDR*

The implementation of Eq. (6) requires calculation of the difference in dip and dip direction between the anisotropy orientation (Dip_j, DDR_j) and the direction of the shear plane (Dip_{SP}, DDR_{SP}). A sliding direction must be assumed to calculate ΔDDR. A downward direction of sliding is assumed for these calculations; this is appropriate for two-dimensional plane strain analysis. The following vectors are used to estimate ΔDip and ΔDDR:

- Vector $\hat{A}$ is a vector normal to the anisotropy plane.
- Vector $\hat{B}$ is a vector normal to the assumed shear plane orientation.
- Vector $\hat{C}$ is the cross product of $\hat{B}$ x (0,0,-1). This is where downward sliding is assumed.
- Vector $\hat{D}$ is $\hat{A}$ rotated around $\hat{C}$ by the dip of the shear plane.
- ΔDip is the arccosine of the dot product of $\hat{A}$ and $\hat{B}$, as shown in Eq. (11).
- ΔDDR is the dip direction of $\hat{D}$, as shown in Eq. (12).

$$\hat{A} = \begin{cases} \sin(DDR_j) * \sin(Dip_j) \\ \cos(DDR_j) * \sin(Dip_j) \\ \cos(Dip_j) \end{cases} \quad (7)$$

$$\hat{B} = \begin{cases} \sin(DDR_{SP}) * \sin(Dip_{SP}) \\ \cos(DDR_{SP}) * \sin(Dip_{SP}) \\ \cos(Dip_{SP}) \end{cases} \quad (8)$$

$$\hat{C} = \begin{cases} -b_2 / \sqrt{{b_1}^2 + {b_2}^2} \\ b_1 / \sqrt{{b_1}^2 + {b_2}^2} \\ - \end{cases} \quad (9)$$

$$\hat{D} = \begin{cases} [1-\cos(-Dip_{SP})] * (a_1c_1 + a_2c_2) * c_1 + a_1 * \cos(-Dip_{SP}) + c_2a_3\sin(-Dip_{SP}) \\ [1-\cos(-Dip_{SP})] * (a_1c_1 + a_2c_2) * c_2 + a_2 * \cos(-Dip_{SP}) - a_3c_1\sin(-Dip_{SP}) \\ - \end{cases} \quad (10)$$

$$\Delta Dip = \text{acos}(a_1b_1 + a_2b_2 + a_3b_3) \quad (11)$$

$$\Delta DDR = \text{atan}\left(\frac{d_2}{d_1}\right), adjusted\ for\ the\ quadrant \quad (12)$$

2.5. *Calculation of Strength Reduction Factors and Combination of Multiple Joint Sets*

The two strength reduction factors, R_J and R_D, are used to calculate a combined reduction factor, R_C, that is used to estimate the anisotropic strength for any three-dimensional direction of shear. The simplest method to combine the factors is to calculate an anisotropic strength parallel to jointing with R_J, and then reduce that strength due to directional difference with R_D. This is equivalent to assuming that the strength reductions are non-mutually exclusive events, as shown in Eq. (13).

$$R_C = R_J + R_D - R_J R_D \quad (13)$$

Rock masses typically contain many joint sets, and therefore many different orientations of anisotropic weakness. To combine the anisotropy from different joint sets into a single reduction factor, R_F, it is assumed that the estimated strength reduction is independent for each joint set, which is the simplest method of combination, as shown in Eq. (14).

$$R_F = R_{C-1} * R_{C-2} * R_{C-3} * \ldots \quad (14)$$

Liu et al. (2017) performed UCS tests with physical samples and with numerical simulations with one, two, three, or four continuous discontinuities at different orientations. The assumption of an independent strength reduction for each separate weakness in the sample (Eq. 14) can be tested with the results, since the strength reduction factor for each discontinuity orientation was tested individually. The results of applying the

independent strength reduction factors are shown in Table 2, and demonstrate good predictive capability of the proposed model.

2.6. Rock-Mass Strength Estimation

To estimate the final anisotropic rock-mass strength ($Coh_{Dip,DDR}$,$tan\Phi_{Dip,DDR}$), a rock-mass bridge strength (Coh_B,$tan\Phi_B$) must be estimated, which is the strength of the rock mass in orientations of shear away from the orientations of anisotropy. The bridge strength will lie between the minimum possible strength, i.e., a continuous joint (Coh_j ,$tan\Phi_j$), and the maximum strength, i.e., the intact rock strength (Coh_i ,$tan\Phi_i$). This strength will be greater than the anisotropy but less than the intact strength since the strength will be degraded by planes of weakness in directions other than the anisotropy. The weighting methodology is shown in Eqs. (15) to (18). Mine sites where high quality and extensive cell mapping data were available were used to calibrate the intact rock weighting factor, R_W, as shown in Figure 5 and Eq. (19). The calibration cases were achieved either through (a) back analysis of displacement, or (b) by modifying the factor until the mean rock-mass strength (average of strength in all directions) was equal to the estimated isotropic rock-mass strength. This may be a conservative method to estimate the weighting factor since isotropic rock-mass strength estimation methods have been calibrated to existing failures, where anisotropy was likely a contributing factor. The endpoint of 0.5 is intuitively reasonable, as this is near the reduction factor that would be expected due to scale effects alone (scaling from the size of a typical UCS core sample to rock-mass scale).

$$Coh_B = R_W * Coh_i + (1 - R_W) * Coh_j \quad (15)$$

$$tan\emptyset_B = \sqrt{R_W} * tan\emptyset_i + \left(1 - \sqrt{R_W}\right) * tan\emptyset_j \quad (16)$$

$$Coh_{Dip,DDR} = R_F * Coh_B + (1 - R_F) * Coh_j \quad (17)$$

$$tan\emptyset_{Dip,DDR} = \sqrt{R_F} * tan\emptyset_B + \left(1 - \sqrt{R_F}\right) * tan\emptyset_j \quad (18)$$

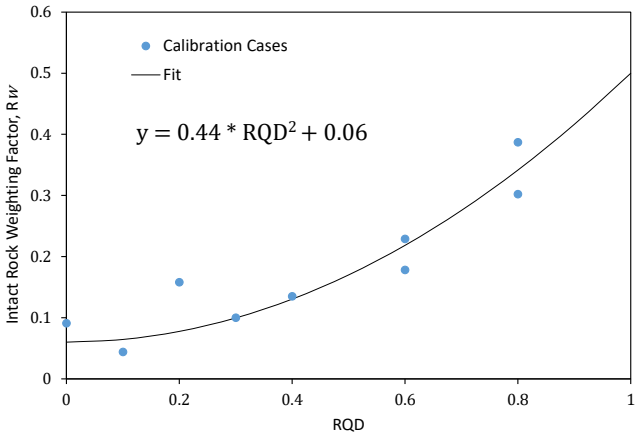

Fig. 5. RQD versus estimated intact rock weighting factor.

$$R_W \approx 0.44 * RQD^2 + 0.06 \quad (19)$$

Table 2. Strength reduction factors from Liu (2017) compared against proposed model

Sample ID	Dip of Joint(s)	UCS (MPa)	Reduction Factor, R_C Measured	Individual Reduction Factors, R_C, Measured	Reduction Factor, Model	Error (Difference)
A1	0	41.0	0.84			
A2	15	39.5	0.79			
A3	30	34.9	0.66			
A4	45	20.7	0.26			
A5	60	13.6	0.06			
A6	75	11.7	0.01			
A7	90	40.1	0.81			
B1	0, 90	36.2	0.70	0.84, 0.81	0.68	-0.02
B2	15, 75	11.8	0.01	0.79, 0.01	0.01	0.00
B3	30, 60	13.5	0.06	0.66, 0.06	0.04	-0.02
B4*	45, 45	20.1	0.24	0.26, 0.26	0.07	-0.18
C1	0, 60	11.7	0.01	0.84, 0.06	0.05	0.04
C2	15, 45, 75	11.6	0.00	0.79, 0.01, 0.26	0.00	0.00
C3	30, 90	22.7	0.32	0.66, 0.81	0.54	0.22
D1	0, 45, 90	17.0	0.16	0.84, 0.26, 0.81	0.18	0.02
D2	15, 45, 60, 75	10.6	0.00	0.79, 0.26, 0.06, 0.01	0.00	0.00

*B4 is expected to have the same UCS as A4 since there was no constraint on the direction of shear plane formation during failure. The assumption of independent strength reduction factors would not be expected to perform well for this case.

3. CALCULATION SPREADSHEET

A worksheet has been created that accommodates up to nine simultaneous discontinuity sets and performs all of the calculations presented herein. The worksheet estimates the strength for any directions of shear and for any cross-section orientation. The worksheet is shown in Figure 6 and is available for public download at the website "https://www.cnitucson.com/publications.html".

3D/2D Anisotropic Strength Estimation Worksheet

Project #	21310	*CALL & NICHOLAS, INC.*		Client	Mine
Date	2/18/2021	*TUCSON, ARIZONA USA*		Location	USA
Engineer	SDC	*Based on: Three-Dimensional Anisotropic Shear Strength of Closely Jointed Rock Masses. In, 55th US Rock Mechanics / Geomechanics Symposium, June 20-23, 2021, Houston, Texas.*		Rock Type	GEOLOGY 6
Comments	Example			Rock Type (2)	Sills

Input Data

			Joint Set	Probability of Occurrence	Dip Direction (deg)	Dip (deg)	Mean Length (ft/m)	Mean Spacing (ft/m)	Strength Reduction Along Joints
Fracture Strength			Joint Set 1	1.00	119	37	5.7	1.8	0.09
Cohesion	34	psf/kPa	Joint Set 2	0.48	156	47	6.1	1.3	0.54
Phi	29.0	deg	Joint Set 3	0.34	181	67	3.4	0.4	0.67
Intact Rock Strength			Joint Set 4	0.91	80	44	4.1	2.5	0.28
Cohesion	8,986	psf/kPa	Joint Set 5	0.43	40	45	3.5	0.7	0.59
Phi	44.9	deg	Joint Set 6	0.33	359	40	4.4	0.4	0.68
Isotropic Rockmass Strength (for reference)			Joint Set 7	0.95	354	73	3.6	0.4	0.07
Cohesion	243	psf/kPa	Joint Set 8	0.69	281	34	3.8	0.5	0.33
Phi	31.7	deg	Joint Set 9	0.36	87	82	2.8	0.4	0.65

RQD: 10% Cross Section Azimuth (Down Dip): 70°

Calculated Values

Intact Rock Weighting Factor	
0.064	
Bridge Strength Between Joints	
Cohesion	610 psf/kPa
Phi	33.7 deg
Mean Anisotropic Rockmass Strength	
Cohesion	169 psf/kPa
Phi	31.2 deg

Structure Data Plot

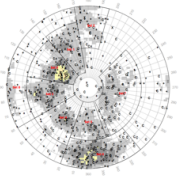

Anisotropic Rockmass Cohesion Plot

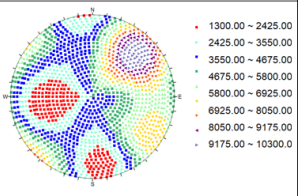

Chart of Anisotropic Cohesion and Phi for Cross Section Strike = 70°

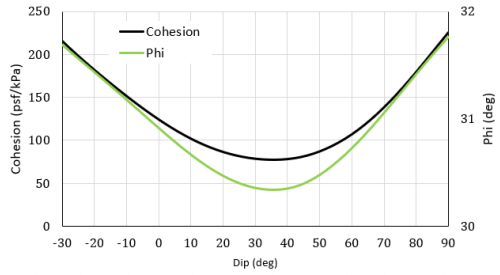

Fig. 6. Anisotropic strength estimation calculation worksheet.

4. EXAMPLES

4.1. Example with One Joint Set

Examples of the anisotropic strength estimation methodology for all potential directions of shear can be seen for one joint set dipping at either 20, 45, or 70 degrees in Figure 7 (for a fracture cohesion of 706 kPa, an intact rock cohesion of 197,000 kPa, and an RQD of 20 percent). The cohesion values are plotted by the assumed direction of shear in 3D on a lower hemisphere equal-area stereonet. As expected, the lowest strength is in the direction of jointing (dip direction of 45 degrees), and the estimated strength increases away from the orientation of the jointing. The contours of cohesion are elongated in the downward direction, as this is the assumed direction of sliding (other directions could be assumed if desired).

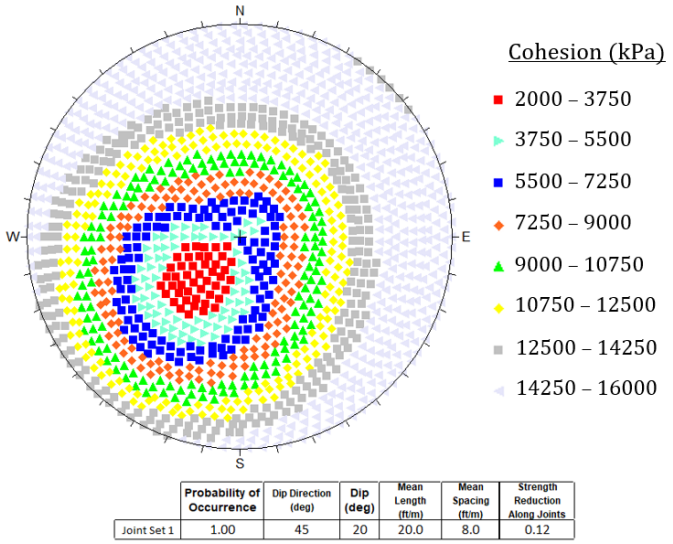

	Probability of Occurrence	Dip Direction (deg)	Dip (deg)	Mean Length (ft/m)	Mean Spacing (ft/m)	Strength Reduction Along Joints
Joint Set 1	1.00	45	20	20.0	8.0	0.12

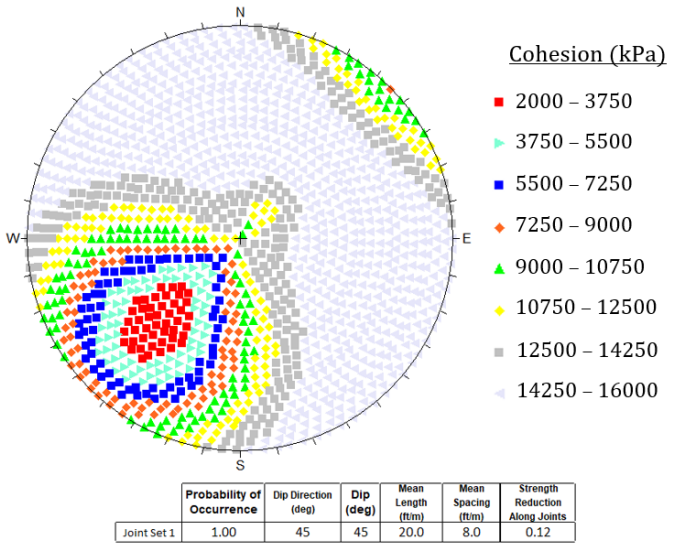

	Probability of Occurrence	Dip Direction (deg)	Dip (deg)	Mean Length (ft/m)	Mean Spacing (ft/m)	Strength Reduction Along Joints
Joint Set 1	1.00	45	45	20.0	8.0	0.12

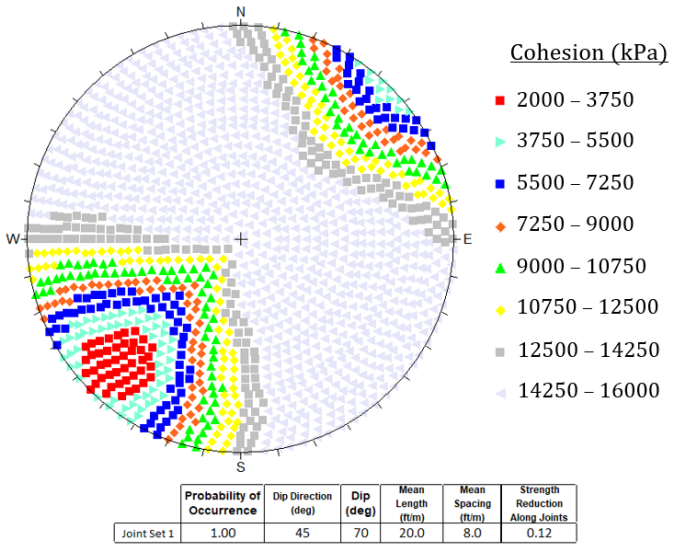

	Probability of Occurrence	Dip Direction (deg)	Dip (deg)	Mean Length (ft/m)	Mean Spacing (ft/m)	Strength Reduction Along Joints
Joint Set 1	1.00	45	70	20.0	8.0	0.12

Fig. 7. Lower hemisphere equal-area stereonets showing estimated rock-mass cohesion for a joint set with a DDR of 45 degrees for dip values of 20, 45, and 70 degrees.

4.2. *Example with Multiple Joint Sets*

An example anisotropic strength estimation can be seen for five simultaneous joint sets in Figure 8, with each joint set pole shown as a black cross. The lowest cohesion values are centered around the joint sets, and the highest strengths are observed at the directions of shear furthest away from jointing.

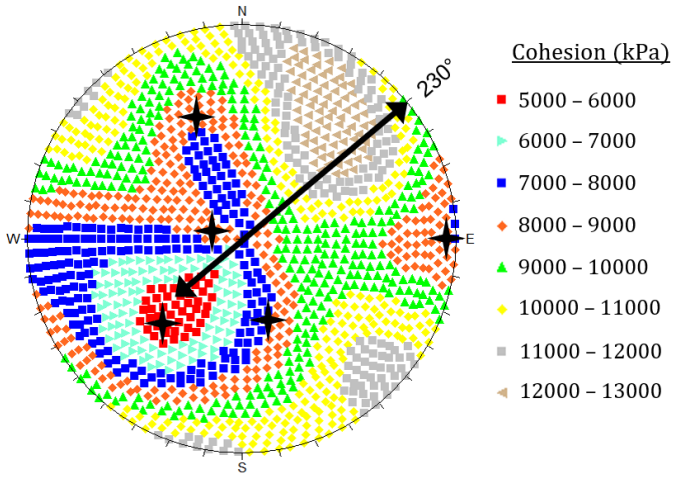

	Probability of Occurrence	Dip Direction (deg)	Dip (deg)	Mean Length (ft/m)	Mean Spacing (ft/m)	Strength Reduction Along Joints
Joint Set 1	0.60	45	45	20.0	4.0	0.43
Joint Set 2	0.20	100	10	10.0	3.0	0.82
Joint Set 3	0.45	160	50	15.0	1.0	0.55
Joint Set 4	0.50	270	85	25.0	3.0	0.51
Joint Set 5	0.40	340	30	12.0	5.0	0.65

Fig. 8. Lower hemisphere equal-area stereonet showing estimated rock-mass cohesion with 5 simulated joint sets.

4.3. *Example Anisotropy Along a Cross Section*

Anisotropic strength can be quickly estimated along any cross-section orientation with the methodology. Figure 9 shows the anisotropic cohesion and friction angle for the five joint sets presented in Figure 8.

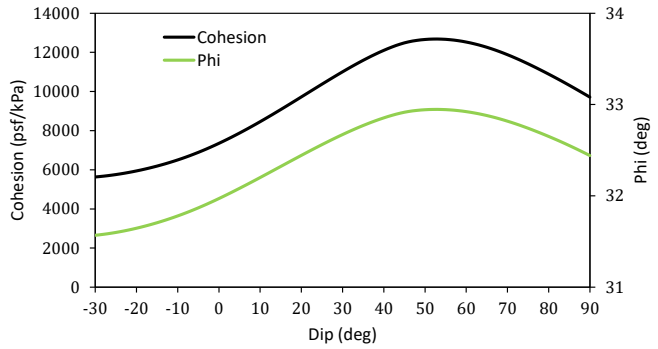

Fig. 9. Estimated anisotropic cohesion and friction angle for cross section strike 230 degrees.

4.4. *Example Slope Stability Analysis*

The anisotropic strength estimation method was used to back analyze a slope failure at a copper porphyry mine in the southwestern United States. The slope height at the time of instability was 105 meters, the interramp slope angle was 38 degrees, and the slope is primarily comprised of granodiorite sills. The wall dip direction is 70 degrees. The joint set cell mapping data for the slope and the shear strength along the azimuth of the cross section are shown in Figure 6. As can be seen, there are many joint sets which may contribute to anisotropic weakness for that wall orientation. The properties of the rock mass are shown in Table 3. A comparison of the estimated Hoek-Brown rock-mass strength (Hoek et al. 2002) and the estimated anisotropic strengths for various dip angles is shown in Figure 10.

Table 3. Properties of the granodiorite sills

	Intact UCS [kPa]	GSI	RQD	m_i	D (damage factor)
Sills	43,260	29	10%	28.10	1.0

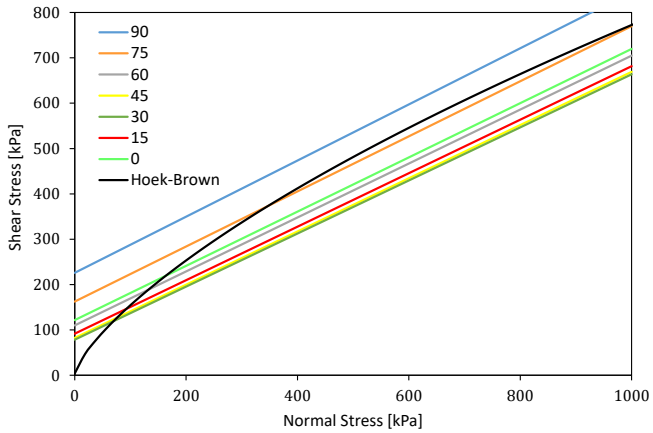

Fig. 10. Comparison of Hoek-Brown rock-mass strength estimate and linear anisotropic strength estimates for various dip angles.

The two-dimensional limit-equilibrium analysis of the slope using Hoek-Brown rock-mass strengths is shown in Figure 11a. The water table surface was estimated from grouted piezometer data. Even with a conservative assumption of a damage factor equal to 1.0, the resulting factor of safety (FOS) value is 1.249. The target FOS value is 1.0 since displacement was experienced on the slope. Isotropic rock-mass strengths are likely inappropriate for this analysis due to the strong jointing sub-parallel to the slope. The analysis with the anisotropic strengths is shown in Figure 11b, and results in a FOS value of 1.056, which is closer to the target back analysis FOS value of 1.0.

5. ADDITIONAL CONSIDERATIONS

- Most of the studies utilized to develop this methodology considered a single orientation of anisotropy. When a rock mass with multiple joint sets is sheared, the behavior of one joint set will be affected by the presence of other joint sets, and this is not considered herein.

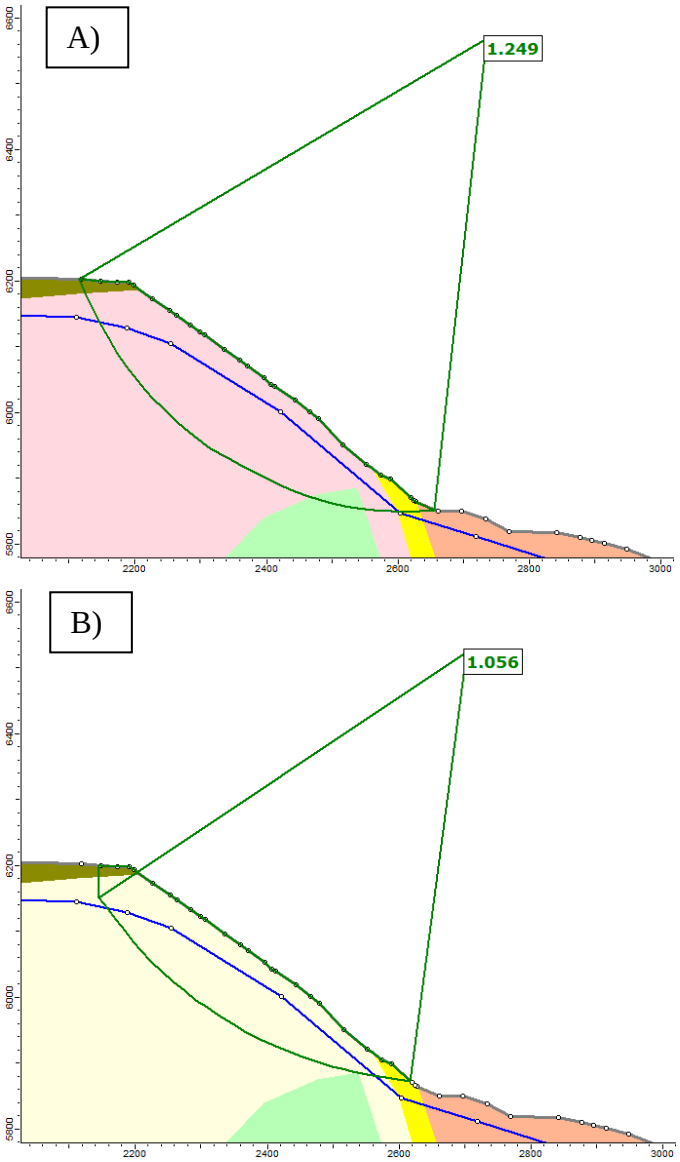

Fig. 11. Comparison of back analysis using (A) Hoek-Brown isotropic strengths and (B) anisotropic strengths. Note: Scale bars are in feet.

- The relation between the shear plane and anisotropy due to jointing is three dimensional. Ideally, the system should be based on three-dimensional vectors and not on the difference between dip and dip direction.
- Many of the studies reported peak strengths, but most back analyses of slope failures are calibrated to a post-peak strength.
- Two different strength reduction factors are combined to estimate rock-mass strength with this methodology. The combination of these two reduction factors has not been explicitly studied by any of the authors. No studies were identified of the effects of non-persistent jointing at a different DDR and dip than the shear plane.
- The implementation of this methodology requires the identification of all joint sets present in a rock mass. Mapping and/or borehole surveys should be carried out at multiple orientations to eliminate blind zones.

6. CONCLUSIONS

Published studies and novel data have been combined to create a practical and easily implemented method of estimating anisotropic rock-mass strength for any direction of shear in three dimensions, considering any number of non-persistent discontinuity sets. The methodology is applicable for any type of co-planar discontinuities that may weaken the rock mass (e.g., fault sets). The procedure for estimation is flexible; any of the equations (e.g., strength reduction as a function of joint persistence) may be interchanged or updated independently if future research produces more compelling results, or the methodology could be applied to non-linear rock strength criteria such as Hoek-Brown. The methodology has been programmed into a spreadsheet and made available for public download (Cylwik, 2021), with the hope that other practitioners may build upon, improve, or further calibrate the methodology.

REFERENCES

1. Bahaaddini, M., G. Sharrock, and B.K. Hebblewhite. 2013. Numerical investigation of the effect of joint geometrical parameters on the mechanical properties of a non-persistent jointed rock mass under uniaxial compression. *Computers and Geotechnics*. 49, 206-225.
2. Bahaaddini, M., P. Hagan, R. Mitra, and B.K. Hebblewhite. 2015. Numerical Study of the Mechanical Behavior of Nonpersistent Jointed Rock Masses. *International Journal of Geomechanics*. 16. 04015035. 10.1061/(ASCE)GM.1943-5622.0000510.
3. Cheng, C., X. Chen, S. Zhang. 2016. Multi-peak deformation behavior of jointed rock mass under uniaxial compression: Insight from particle flow modeling. *Engineering Geology*. 213: 25-45.
4. Cylwik, S.D. "3D/2D Anisotropic Strength Estimation Worksheet." Call & Nicholas, 22 April 2021, https://www.cnitucson.com/publications.html.
5. Fereshtenejad, S. Fundamental Study on Shear Behavior of Non-Persistent Joints. Ph.D. Thesis, Seoul National University, Seoul, Korea, 2020.
6. Hoek, E., C. Carranza-Torres, B. Corkum. 2002. Hoek-Brown failure criterion – 2002 edition, in *Proceedings of the Fifth North American Rock Mechanics Symposium*, Hammah et al. (eds), University of Toronto Press, pp.267-273.
7. Hu, J., S. Li, H. Liu, L. Li, S. Shi, and C. Qin. 2020. New Modified Model for Estimating the Peak Shear Strength of Rock Mass Containing Nonconsecutive Joint Based

on a Simulated Experiment. *International Journal of Geomechanics*. 20.04020091. 10.1061/(ASCE)GM.1943-5622.0001732.

8. Jennings, J.E. 1972. An approach to the stability of rock slopes based on the theory of limiting equilibrium with a material exhibiting anisotropic shear strength. In *Stability of Rock Slopes. Proceedings of the 13th US Symposium on Rock Mechanics* (ed. E.J. Cording), Urbana, Illinois, pp. 269-302. ASCE, New York.

9. Liu, J, S. Sun, L. Yue, J. Wei, and J. Wu. 2017. Mechanical and failure characteristics of rock-like material with multiple crossed joint sets under uniaxial compression. *Advances in Mechanical Engineering*. 9(7): 1-18.

10. Nicholas, D.E. and D.B. Sims. 2000. Collecting and Using Geologic Structure Data for Slope Design in *Slope Stability in Surface Mining*. W.A. Hustrulid. Ed., Soc. for Mining, Metallurgy, and Exploration, Inc: Littleton, Colorado.

11. Shaunik, D. and M. Singh. 2019. Strength behaviour of a model rock intersected by non-persistent joint. *Journal of Rock Mechanics and Geotechnical Engineering*. 11(6). 1243-1255.